MICROBIOLOGY

Commensal *Cutibacterium acnes* induce epidermal lipid synthesis important for skin barrier function

Samia Almoughrabie[1,2]*, Laura Cau[2], Kellen Cavagnero[1], Alan M. O'Neill[1], Fengwu Li[1], Andrea Roso-Mares[1], Carine Mainzer[2], Brigitte Closs[2], Matthew J. Kolar[1], Kevin J. Williams[3,4], Steven J. Bensinger[4,5,6], Richard L. Gallo[1]*

Lipid synthesis is necessary for formation of epithelial barriers and homeostasis with external microbes. An analysis of the response of human keratinocytes to several different commensal bacteria on the skin revealed that *Cutibacterium acnes* induced a large increase in essential lipids including triglycerides, ceramides, cholesterol, and free fatty acids. A similar response occurred in mouse epidermis and in human skin affected with acne. Further analysis showed that this increase in lipids was mediated by short-chain fatty acids produced by *Cutibacterium acnes* and was dependent on increased expression of several lipid synthesis genes including *glycerol-3-phosphate-acyltransferase-3*. Inhibition or RNA silencing of peroxisome proliferator–activated receptor–α (PPARα), but not PPARβ and PPARγ, blocked this response. The increase in keratinocyte lipid content improved innate barrier functions including antimicrobial activity, paracellular diffusion, and transepidermal water loss. These results reveal that metabolites from a common commensal bacterium have a previously unappreciated influence on the composition of epidermal lipids.

INTRODUCTION

Epithelial surfaces form an essential barrier between the external milieu and the host. The skin barrier has multiple functions that include temperature regulation and control of the loss of water and electrolytes. Furthermore, epithelial surfaces such as the skin must also permit colonization by a beneficial microbiome and protect against infection by pathogens (*1*–*3*). To achieve this complex function, the synthesis of lipids in the skin by keratinocytes is essential and is assembled in the stratum corneum. In the stratum corneum, corneocytes are surrounded by a neutral lipid-enriched extracellular matrix mainly composed of ceramides, cholesterol, and free fatty acids (*4*, *5*). Disturbances in the composition and/or organization of epidermal lipids can lead to a range of skin diseases including atopic dermatitis, lamellar ichthyosis, and psoriasis (*6*–*9*). Lipid composition on the skin also provides an important antimicrobial shield. However, it is not well understood if the skin microbiome influences the epidermal lipid barrier or if the production of epidermal lipids plays a dynamic role in response to microbial signals.

There are several species of bacteria that normally survive on human skin. *Cutibacterium acnes* (*C. acnes*) is the most common commensal bacterial species on the skin barrier (*10*, *11*) and is an opportunistic pathobiont that is thought to play a major role in the development of acne vulgaris, a common skin disorder of the pilosebaceous unit (*12*). The functions of *C. acnes* to influence skin health have not been extensively studied, but it has been reported to stimulate proinflammatory cytokine and chemokine expression as well as influence sebocyte differentiation and viability (*13*–*15*). *C. acnes* is also known to metabolize free fatty acids from sebum and decrease the surface pH and may thus contribute to barrier homeostasis as this acidic environment helps to inhibit pathogenic bacteria such as *Staphylococcus aureus* while favoring other healthy commensal bacteria (*16*). Short-chain fatty acids (SCFAs) produced by *C. acnes* can also limit the overabundance of *Staphylococcus epidermidis* by inhibiting its biofilm formation (*17*). Overall, the complex interplay between microbes and host is an area of intense research with major implications to health and disease but remains poorly understood.

The influence of the cutaneous microbiota on keratinocyte lipid synthesis has not been extensively studied despite the important role that lipids play in the barrier and the beneficial functions that have been demonstrated for the skin microbiome (*18*, *19*). In this study, we show how SCFAs produced by *C. acnes* modify keratinocyte lipid synthesis and alter epidermal lipid composition to enhance the function of the skin barrier. These observations reveal an important mechanism through which the skin responds to the external environment.

RESULTS

C. acnes induces increased lipid staining in mouse and human skin

In this study, we investigated whether the presence of skin commensal bacteria could influence the production of lipids by the keratinocytes in the epidermis, an essential component of the skin barrier (*4*, *20*, *21*). To test this, normal neonatal human epidermal keratinocytes (NHEKs) were treated with sterile filtrate of conditioned media (CM) from bacterial species commonly found on human skin. Oil Red O (ORO) staining was used to first quantify relative changes in total lipid accumulation and showed that of the species and strains tested here, only *C. acnes* CM could induce a lipid increase in NHEKs (Fig. 1A). The observed increase in lipid staining of NHEKs occurred with CM from multiple different

[1]Department of Dermatology, University of California San Diego, La Jolla CA, USA. [2]SILAB, Brive, France. [3]Department of Biological Chemistry, UCLA, Los Angeles, CA, USA. [4]UCLA Lipidomics Lab, UCLA, Los Angeles, CA, USA. [5]Department of Microbiology, Immunology, and Molecular Genetics, UCLA, Los Angeles, CA, USA. [6]Department of Molecular and Medical Pharmacology, UCLA, Los Angeles, CA, USA.
*Corresponding author. Email: rgallo@health.ucsd.edu (R.L.G.); salmoughrabie@health.ucsd.edu (S.A.)

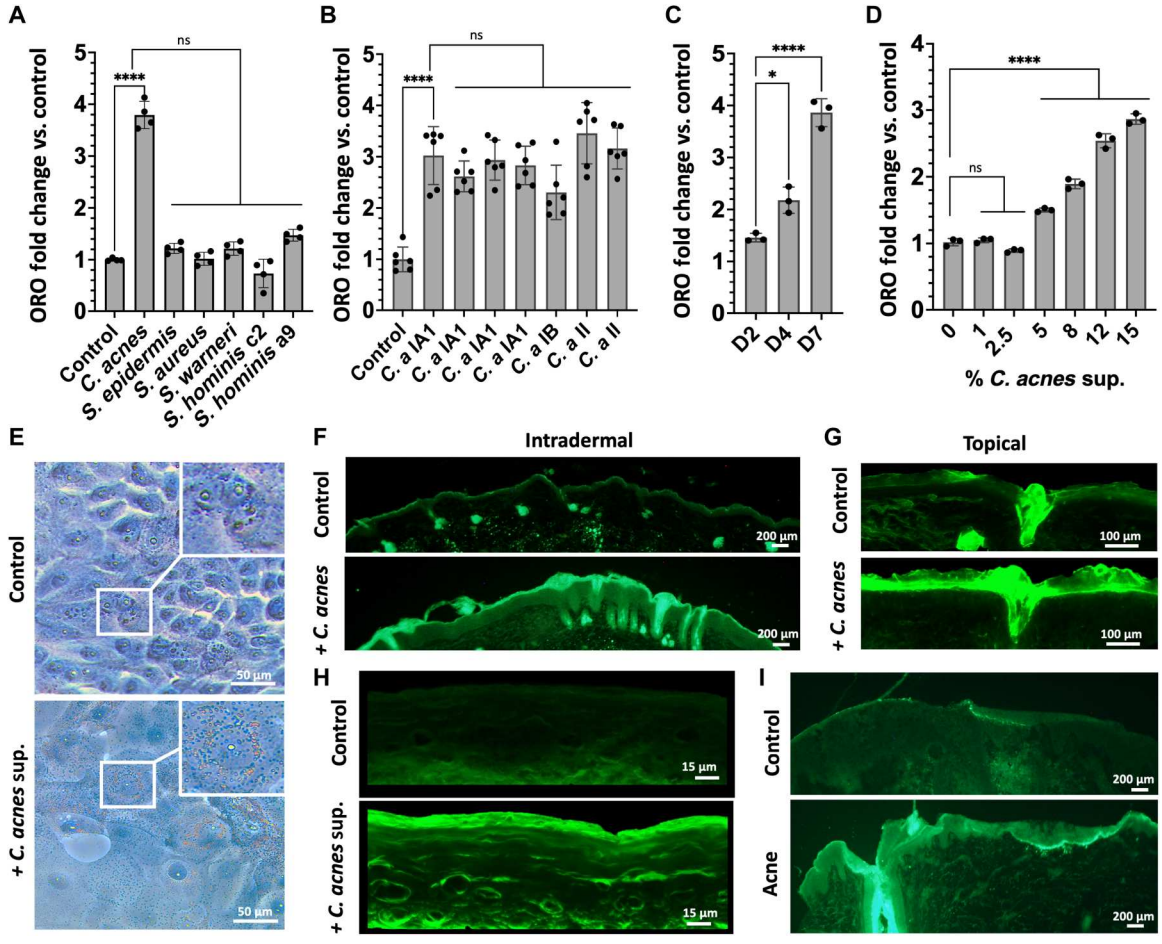

Fig. 1. *C. acnes* induces increased lipid staining in mouse and human skin. (**A**) Oil Red O staining (ORO) of total lipids in NHEKs after treatment with sterile supernatants from media conditioned by the growth of different species of bacteria commonly found on human skin or (**B**) different *C. acnes* strains (*C. a*). (**C**) Oil Red O quantification of total lipids in NHEKs at days 2 (D2), 4 (D4), and 7 (D7) after exposure to 15% of sterile supernatant from *C. acnes* CM. (**D**) Dose-response at day 4 Oil Red O staining of total lipids in NHEK after treatment with different concentrations of sterile supernatant from *C. acnes* conditioned culture media. (**E**) Oil Red O lipid staining of NHEKs with and without sterile supernatant from *C. acnes* conditioned culture media. (**F**) Bodipy lipid staining of mouse skin after intradermal injection of 10^7 CFU/ml of *C. acnes* or (**G**) topical application of 10^7 CFU/cm^2 of *C. acnes* on mice. (**H**) Bodipy lipid staining of reconstructed human epidermis treated with or without sterile supernatant from *C. acnes* CM. (**I**) Bodipy lipid staining of an acne lesion and nonlesional human skin. Experiments conducted were performed at least in triplicate. Not significant (ns) = $P > 0.05$, *$P < 0.05$, ****$P < 0.0001$.

strains of *C. acnes* regardless of the phylotypes tested (Fig. 1B). Lipid accumulation in NHEKs increased with time of exposure to CM (Fig. 1C) and was dose dependent (Fig. 1D). Visualization of Oil Red O staining of NHEKs is shown in Fig. 1E. To assess whether this response could also be observed by keratinocytes in vivo, the back skin of mice was challenged with intradermal injection or topical application of live *C. acnes* and lipid accumulation visualized by Bodipy staining of the epidermis. Both topical and intradermal exposure to *C. acnes* increased lipid staining in the epidermis of mice (Fig. 1, F and G). Similarly, cultured NHEKs grown as an epidermal construct responded to the addition of *C. acnes* CM with an increase in lipid staining (Fig. 1H). The treatment of *C. acnes* CM also increased the level of loricrin and filaggrin in the human reconstructed epidermis (fig. S1, A to C). Last, skin biopsies of acne lesions from humans were evaluated as *C. acnes* is considered the major bacterial species driving this disease. Acne lesions stained by Bodipy also showed a large increase in lipid staining in the epidermis when compared to normal skin used as a control (Fig. 1I). These observations suggest that epidermal keratinocytes increase lipid accumulation in response to *C. acnes*.

C. acnes induces an increase of triglycerides in mice and human keratinocytes

To further validate the observations of lipid accumulation in cultured cells and in skin, we next applied differential mobility spectrometry (DMS)–based shotgun lipidomics to both cultured NHEKs and mouse epidermis exposed to *C. acnes*. Analysis of NHEK lipid composition showed increases in total triacylglycerol (TAG), ceramides, cholesterol esters, and free fatty acids, with the greatest increase seen after 7 days of culture (Fig. 2A and fig. S2A). TAGs were most abundantly increased and occurred in both NHEK cultured with *C. acnes* CM and mouse epidermis exposed to live *C. acnes* (Fig. 2, A to C and E, and fig. S2B). TAGs containing (16:0), (18:1), and (18:2) fatty acids were

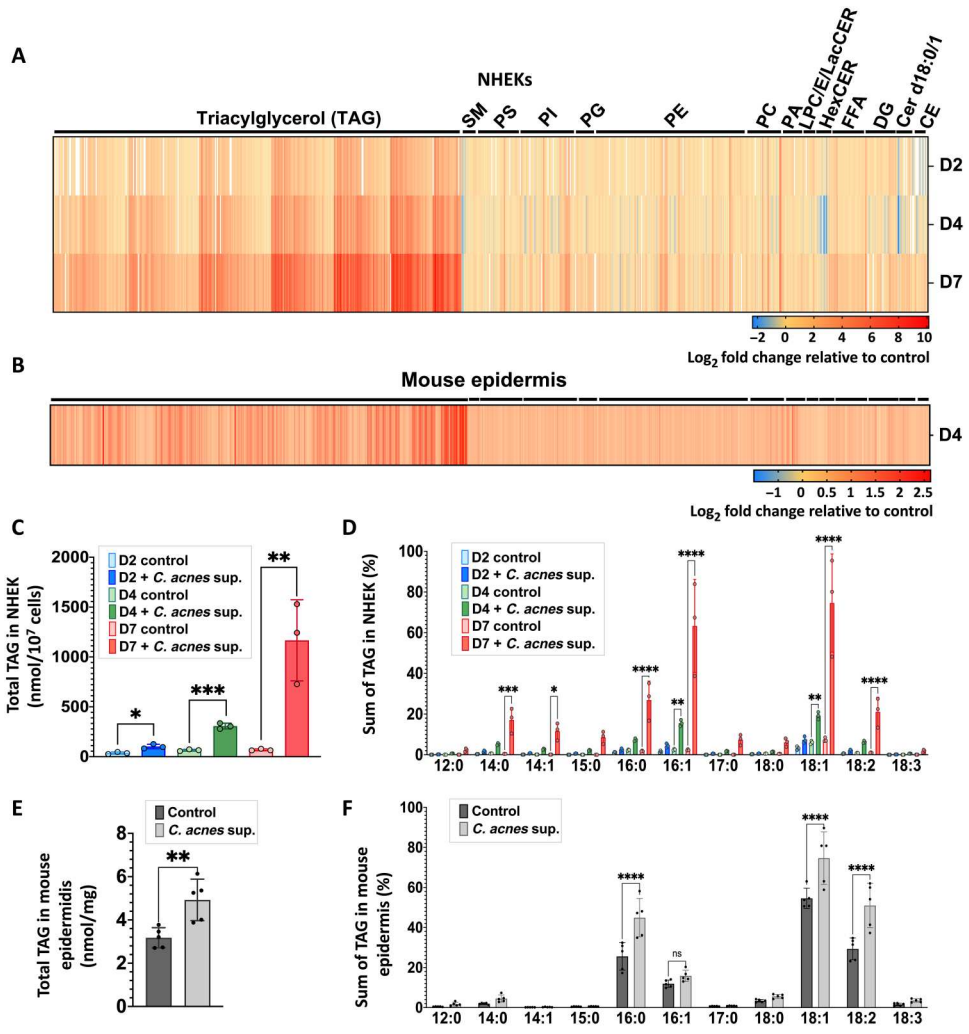

Fig. 2. *C. acnes* induces an increase of triglycerides in mice and human keratinocytes. (**A**) DMS-based shotgun lipidomic analysis of extracted lipids from normal NHEKs after exposure of *C. acnes* CM for 2, 4, and 7 days ($n = 3$) and (**B**) from mouse epidermis exposed to live *C. acnes* at day 4 ($n = 6$). (**C**) Total TAG content in NHEKs and (**E**) in mouse skin treated as in (A) and (B). (**D**) Fatty acid composition analysis of TAG from NHEK and (**F**) from mouse epidermis treated as in (A) and (B). CE, cholesterol esters; Cer d18:1, ceramides; DG, diacylglycerols; Cer d18:0, dihydroceramides; FFA, free fatty acids; HexCER, hexosyl ceramides; LacCER, lactosyl ceramides; LPC, lysophosphatidylcholine; LPE, lysophosphatidylethanolamine; PA, phosphatidic acid; PC, phosphatidylcholine; PE, phosphatidylethanolamine; PG, phosphatidylglycerol; PI, phosphatidylinositol; PS, phosphatidylserine; SM, sphingomyelin. Lipidomic analysis has been performed in triplicate for each time point in NHEKs and in six replicates in mouse epidermis. *$P < 0.05$, **$P < 0.01$, ***$P < 0.001$, ****$P < 0.0001$.

notably increased in both the epidermis and in NHEKs (Fig. 2, D and F). Other TAGs containing (14:0), (14:1), and (16:1) fatty acids increased significantly in NHEKs only (Fig. 2D). TAGs containing two to three double bonds increased most in NHEKs, while no significant changes were found in the whole mouse epidermis (fig. S2, C and D). TAGs with a total chain length of 52 or 54 carbons increased significantly in both NHEKs and in mouse epidermis (fig. S2, E and F). This lipidomic analysis suggested that the common increase in lipid staining observed in cultured keratinocytes and the mouse epidermis was likely to be due to the increase in TAGs containing (16:0), (18:1), and (18:2) fatty acids with a chain length of 52 or 54 carbons.

SCFAs produced by *C. acnes* induces lipid accumulation in keratinocytes

To investigate the mechanism by which *C. acnes* increased lipid accumulation by keratinocytes, we next studied the biochemical properties of *C. acnes* CM that were associated with the capacity to induce lipids. We tested total proteins of *C. acnes* supernatant precipitated with ammonium sulfate and the purified Toll-like receptor 2/6 ligand macrophage-activating lipopeptide-2 (MALP-2). The effect of pH was also assessed as *C. acnes* CM was observed to acidify culture media to pH 7.1. The protein precipitate and the other conditions tested did not induce an increase of lipids in NHEKs (Fig. 3A). During further analysis, the activity of *C. acnes* CM to promote lipid accumulation in NHEKs was observed to be lost after lyophilization, suggesting that the activity was from volatile molecules present in the *C. acnes* CM (Fig. 3B). Since SCFAs are a

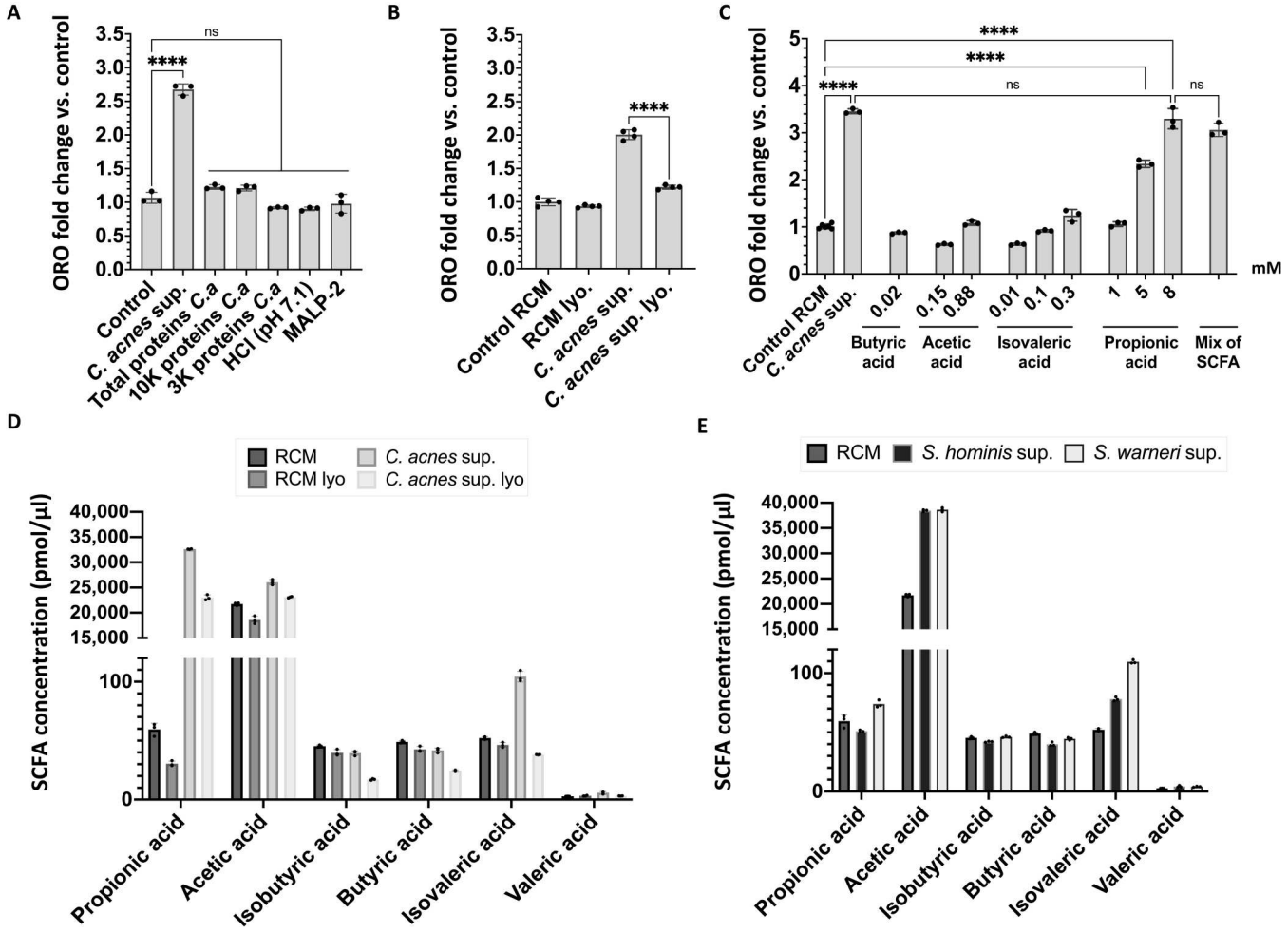

Fig. 3. Propionic acid produced by *C. acnes* induces lipid accumulation in keratinocytes. (**A**) Oil Red O quantification at day 4 in NHEKs after adding sterile CM from *C. acnes* supernatant (*C.a*) or proteins from *C. acnes* media precipitated with ammonium sulfate (85% saturation) or ultrafiltrates from *C. acnes* media at less than 10 and 3 kDa or media adjusted to pH 7.1 with hydrochloric acid (HCl) or Malp-2 (100 ng/ml). (**B**) Oil Red O quantification of NHEK at day 4 after adding 15% of *C. acnes* conditioned culture media supernatant or media control without *C. acnes* [reinforced clostridial medium (RCM)] or *C. acnes* CM after lyophilization (lyo.) or nonlyophilized. (**C**) Oil Red O quantification of NHEK at day 4 after adding different concentration of SCFA alone or in a mix containing 8 mM propionic acid, 0.6 mM acetic acid, 0.01 mM isovaleric acid, and 0.02 mM butyric acid. (**D** and **E**) SCFA composition of bacterial supernatants by gas chromatography–mass spectrometry. Experiments conducted were performed at least in triplicate. ****$P < 0.0001$.

predominant class of volatile compounds produced during the culture of *C. acnes* (*13*), we then tested several purified SCFAs for their capacity to increase lipids in NHEKs. Butyric acid, acetic acid, and isovaleric acid did not induce a significant increase in NHEK lipids, whereas propionic acid (PA) induced a level of lipid accumulation similar to that seen when NHEKs are exposed to *C. acnes* CM (Fig. 3C). We have also tested the possibility of a combination of PA with the others SCFA to induce the increase of lipid synthesis in NHEKs and did not observe any significant difference compared to PA alone (Fig. 3C). Liquid chromatography–mass spectrometry (LC-MS) analysis of the SCFA composition in *C. acnes* CM before and after lyophilization showed that lyophilization of the *C. acnes* CM led to a 30% decrease in propionic acid concentration (Fig. 3D). The concentration of other SCFAs also decreased after lyophilization, but propionic acid decreased the most (loss of around 10,000 pmol/µl) (Fig. 3D). Other human skin commensal bacteria, including two species of *Staphylococcus*, had a low concentration of propionic acid in comparison to *C. acnes* supernatant (Fig. 3E). Together, these observations suggested that the production of the SCFA by *C. acnes* can induce lipid accumulation in keratinocytes.

C. acnes and propionic acid increase expression of lipid synthesis genes in keratinocytes

We next evaluated the effects of *C. acnes* CM or propionic acid on gene expression in NHEKs. RNA sequencing (RNA-seq) analysis of NHEKs exposed to *C. acnes* CM or propionic acid showed related global changes (Fig. 4A). Principal components analysis (PCA) showed that *C. acnes* CM and propionic acid induced that were not identical but correlated well at PC1 with represented 90% of the variance (Fig. 4B). Heatmap analysis of genes involved in lipid synthesis showed increased expression several genes and similar responses when stimulated with *C. acnes* supernatant or propionic acid (Fig. 4C). These observations were validated by

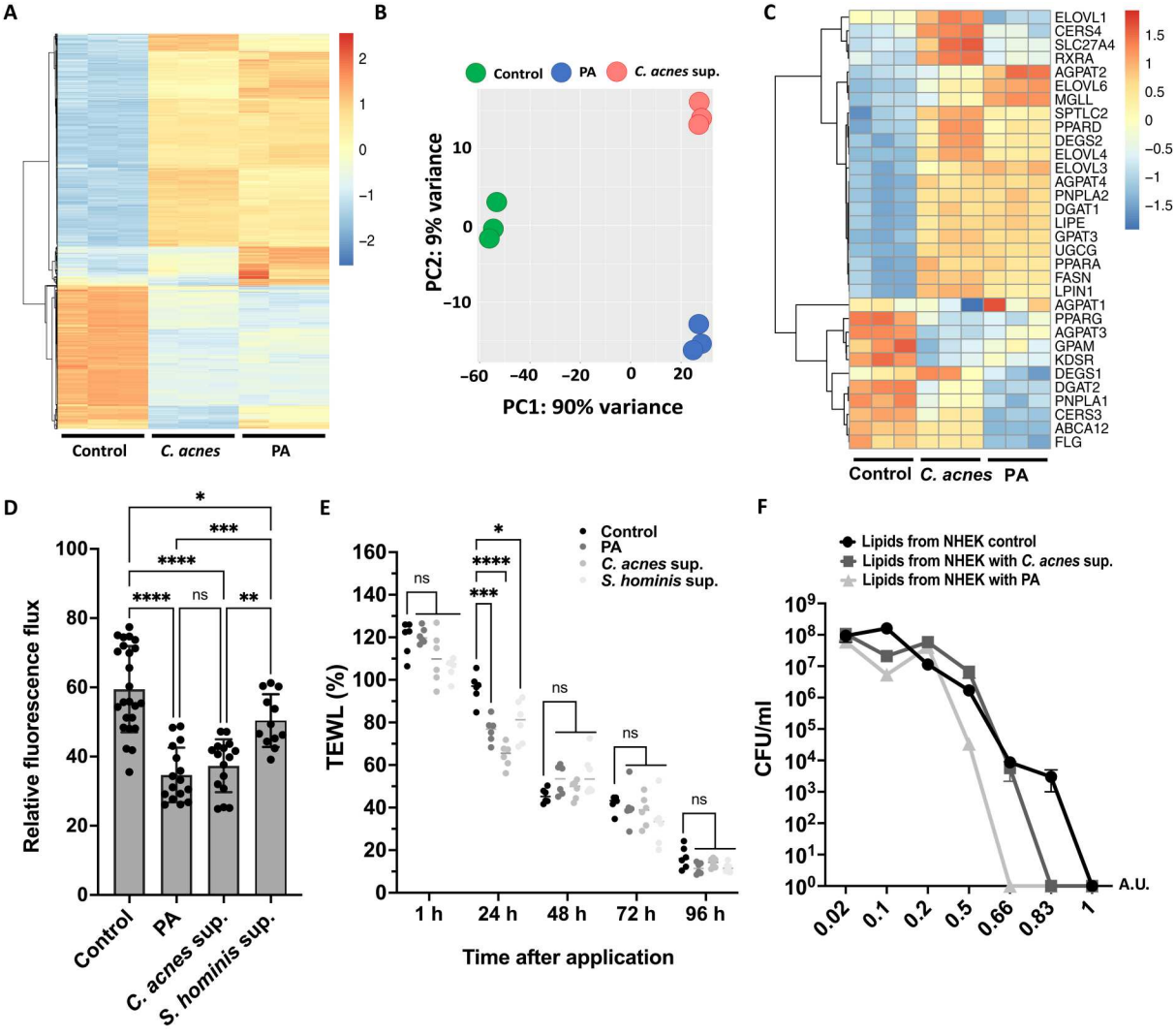

Fig. 4. *C. acnes* and propionic acid increase expression of lipid synthesis genes and enhance the barrier and the antimicrobial function of keratinocytes. (**A**) RNA-seq heatmap showing the top 2000 genes differentially expressed in NHEKs in response to exposure to 15% of *C. acnes* CM or 8 mM propionic acid for 4 days. (**B**) PCA of the normalized RNA-seq data. (**C**) Heatmap showing effect of *C. acnes* CM or propionic acid (PA) on genes involved in the lipid. (**D**) Paracellular diffusion of FD-4 solution (1.25 mg/ml) after exposure of confluent NHEK to 8 mM propionic acid or 15% of *C. acnes* supernatant or *S. hominis* supernatant. (**E**) Transepidermal water loss (TEWL) on tape-stripped mouse skin after applying *C. acnes* supernatant or 8 mM propionic acid topically. (**F**) Growth curves of *C. acnes* treated with different concentrations of lipids extracted from NHEK after exposing to 15% *C. acnes* supernatant or 8 mM propionic acid for 4 days. Note that the heatmaps were scaled by row. Experiments conducted were performed at least in triplicate. A.U., arbitrary unit. *P < 0.05, **P < 0.01, ***P < 0.001, and ****P < 0.0001.

quantitative polymerase chain reaction (qPCR), which showed a similar global increase in many genes involved in lipid synthesis after exposure to either *C. acnes* CM or propionic acid (fig. S3). However, the gene expression analysis showed a reduction in the expression of loricrin and filaggrin in NHEKs, which appears to be different from the results observed in a three-dimensional model of a human reconstructed epidermis where an increase in the production of these proteins was observed (fig. S1).

C. acnes enhances the barrier and antimicrobial function of keratinocytes

To confirm that changes in lipid accumulation by keratinocytes after exposure to *C. acnes* would have the expected changes in epithelial function, we measured physical barrier properties of keratinocyte monolayers and in skin mice, as well as the host defense activity of extracted lipids. Transepithelial permeability of cultured NHEKs was assessed by paracellular diffusion of FD-4 (Fluorescein isothiocyanate–dextran) (*22*). NHEKs exposed to *C. acnes* CM had a decrease in the relative flux of FD-4 compared to the control, suggesting an improvement in epidermal permeability barrier function (Fig. 4D). After applying *C. acnes* supernatant or 8 mM propionic acid topically on tape-stripped mouse skin, the measurement of transepidermal water loss (TEWL) showed a significant improvement in skin permeability after just 1 day compared to the control (Fig. 4E). Treatment with *Staphylococcus hominis* CM led to a modest enhancement in epidermal permeability barrier function, indicated by a slight decrease in the relative flux of FD-4 (Fig. 4D) and in TEWL (Fig. 4E). However, the observed reduction was not as

substantial as that observed with *C. acnes* supernatant or propionic acid. Next, total lipids were extracted from identical numbers of NHEKs after *C. acnes* CM or propionic acid exposure. Addition of this lipid extract to growing cultures of live *C. acnes* showed that the potency of antimicrobial activity from NHEKs lipids was increased from cells treated with either *C. acnes* CM or propionic acid (Fig. 4F). Lipids extracted from NHEKs after propionic acid treatment induced the greatest inhibition, correlating with a higher concentration of PA than in the *C. acnes* supernatant (8 mM versus 5 mM according to the concentration given by LC-MS in Fig. 3D). These findings confirmed prior observations that lipids produced by keratinocytes influence barrier functions and are antimicrobial. This therefore supported the hypothesis that keratinocyte function is changed following the increase in lipids induced by *C. acnes*.

Lipid induction by propionic acid involves peroxisome proliferator–activated receptors and the activity of GPAT3

Having established that propionic acid can induce keratinocyte lipid accumulation and transcription of lipid synthesis genes, we next sought to better understand the underlying mechanisms responsible for this increase. Previous reports have shown that the SCFA butyrate can bind and activate peroxisome proliferator–activated receptor–γ (PPARγ) receptors in colonocytes (*23*) and that PPARs can influence lipid synthesis. Therefore, we hypothesized that *C. acnes* could act through PPARs in keratinocytes. Inhibition of PPARα blocked an increase in total lipid by *C. acnes*, whereas inhibition of PPARβ and PPARγ did not (Fig. 5, A and B). Inhibition of PPARα also inhibited expression of *GPAT3* and *FASN* but not *UGCG* as measured by qPCR (Fig. 5C and fig. S4, A and B). Additional evidence for the role of PPARα to mediate the activity of propionic acid was obtained by using small interfering RNA (siRNA) to knock down *PPAR*s in NHEKs. Similar to the response to chemical inhibitors of PPARs, silencing of *PPARα* decreased the capacity of *C. acnes* CM or propionic acid to induce lipid accumulation and expression of the lipid synthesis genes *GPAT3* but not *FASN* and *UGCG*, but silencing of *PPARβ/δ* did not (fig. S5, A to D). Silencing of *PPARγ* led to off-target effects on the expression of *PPARα* and *PPARβ/δ* (fig. S7, A to C).

Since *GPAT3* is important for triglyceride synthesis (*24*) and *GPAT3* was dependent on PPARα, *GPAT3* was targeted to test its role in lipid accumulation. siRNA partially inhibited *GPAT3* (fig. S7D) and resulted in a decrease of lipid accumulation measured by Oil Red O staining in NHEK after stimulation by *C. acnes* CM or propionic acid (Fig. 5D). The role of the free fatty acid receptors GPR41/FFAR3 and GPR43/FFAR2 have been also investigated as previous studies have showed that SCFAs can interact with these cell surface G protein–coupled receptors (*13*, *25*). However, silencing of *FFAR2* or *FFAR3* did not decrease the capacity of *C. acnes* CM or PA to induce lipid production in NHEKs and expression of *GPAT3*, *FASN*, and *UGCG* (figs. S6, A to D, and S7, E and F). Together, these results provide a model to illustrate the mechanism responsible for increased lipid accumulation in NHEKs after exposure to *C. acnes* (Fig. 6).

DISCUSSION

C. acnes is the most abundant bacterial species on human skin, and although it has been associated with inflammatory skin diseases such as acne vulgaris, the significance of its colonization on healthy human skin has been unclear. Our study shows that metabolic products of *C. acnes* induce keratinocytes to increase lipid synthesis, with a large increase seen predominantly in TAGs. Our data also show that *C. acnes* can mediate this effect through its production of propionic acid and subsequent activation of keratinocyte PPARα. The changes observed by this mechanism in lipid accumulation influence the permeability properties in vitro and in vivo and also the antimicrobial activity of the epidermis, thus suggesting that this commensal organism may benefit skin function by enhancing barrier function and limiting bacterial proliferation. This finding provides insight into how the skin microbiome can contribute to epidermal homeostasis.

Although our observations show that TAGs were most abundantly induced by *C. acnes*, TAGs are a minor component of lamellar bodies in the stratum corneum, and their role in epidermal homeostasis is poorly defined (*18*). Supportive evidence for a critical role for TAGs in the skin barrier is seen in human disorders of triglyceride metabolism such as ABHD5/CGI-58 (αβhydrolase domain containing 5, lysophosphatidic acid acyltransferase), PNPLA2 (patatin like phospholipase domain containing 2), and DGAT2 (acyl-CoA:diacylglycerol acyltransferase-2), which lead to severe skin permeability barrier dysfunction and malformation of the cornified lipid envelope due to increased dehydration and a lack of ω-(*O*)-acylceramides (*26*–*29*). It has also been reported that patients with atopic dermatitis have a decrease of *C. acnes* and a decrease of TAG46:2, TAG48:2, TAG50:2, and TAG50:3 that correlates with higher TEWL (*30*). We observed that these TAGs (TAG46, TAG48, and TAG50) were increased with increased exposure to *C. acnes*. A positive effect of TAGs on epidermal permeability function could reflect a breakdown of TAG to provide fatty acids required for the synthesis of ceramide, a crucial lipid for function of the permeability barrier. One potential example is linoleic acid (18:2), a fatty acid required for acylceramide synthesis and essential for corneocyte lipid envelope formation (*21*). This fatty acid is decreased in the epidermis in patients with ichthyosis (*31*), and acne-prone patients have low concentrations of linoleic acid and a relative lack of ceramide (*32*, *33*). In our study, lipidomic analyses showed an increase of triglycerides containing linolenic acid (TAG18:2) and an increase of total ceramide in NHEKs after *C. acnes* exposure. These observations suggest that linoleic acid may be hydrolyzed from TAG and then contribute to acylceramide synthesis to maintain skin barrier function. In disease states such as acne, one could speculate that the host response to *C. acnes* is decreased, leading to lesser linoleic acid and a weakened barrier that enables invasion at the follicle and the acute inflammation associated with disease. If this is the case, then our observations of increased lipid staining in acne may reflect the resolution phase of the disorder.

In our study, we have not specifically identified the antimicrobial lipids induced by keratinocytes in response to *C. acnes*, but we showed that total lipid extracted from NHEKs after exposure to *C. acnes* CM or propionic acid has increased antimicrobial potency against *C. acnes*. This increase in antimicrobial activity can likely be attributed to the lipids extracted from NHEKs rather than propionic acid since the methanol/chloroform extraction of lipid from NHEK removes the chloroform phase through drying, thus minimizing the presence of volatile SCFAs like propionic acid. Many lipids potentially made by NHEK have antimicrobial activity

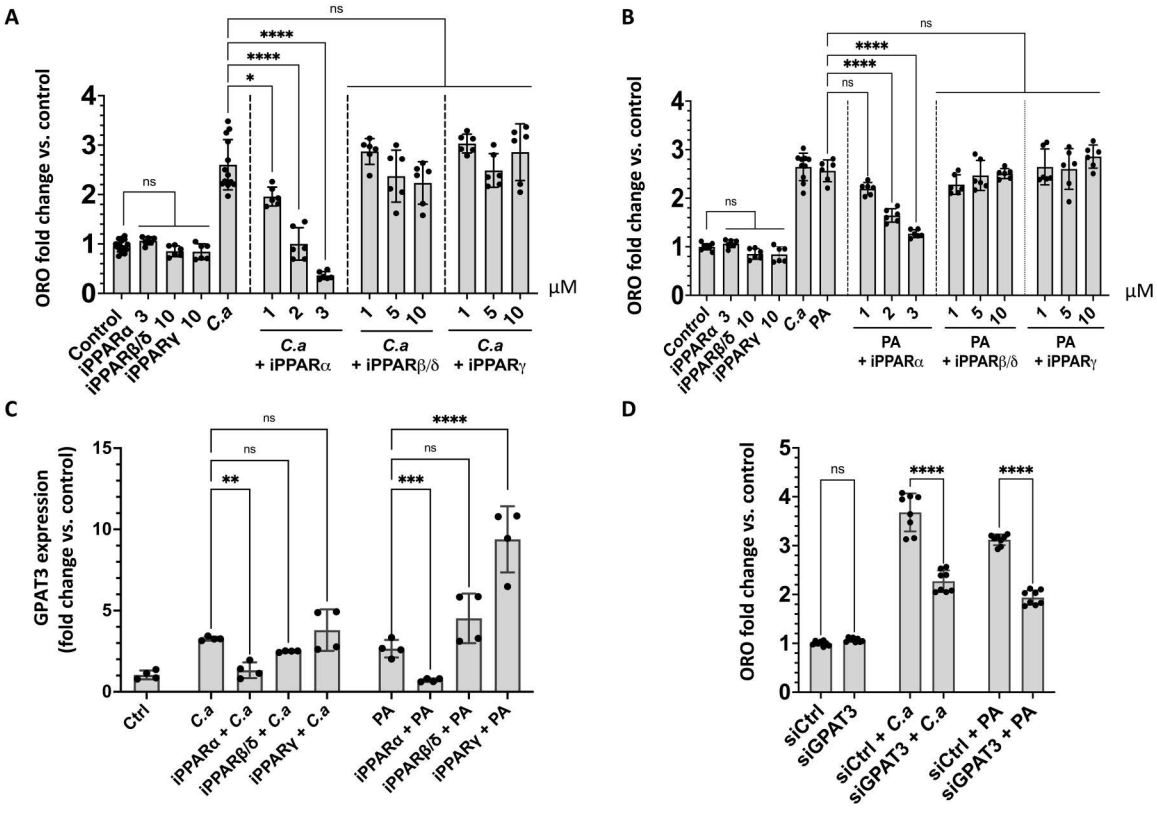

Fig. 5. Lipid induction by propionic acid involves PPARs and the activity of GPAT3. (**A**) Oil Red O lipid quantification in NHEKs after exposure to sterile conditioned *C. acnes* supernatant (*C.a*) or (**B**) of 8 mM propionic acid (PA) with different concentrations of inhibitors for PPARα (GW6471), PPARβ/δ (GSK3787), and PPARγ (T0070907). (**C**) Expression of *GPAT3* measured by qPCR in NHEKs after adding 15% *C. acnes* supernatant (*C.a*) or 8 mM PA and PPARα inhibitor at 3 μM or PPARβ/δ and PPARγ inhibitors at 10 μM (**D**) Oil Red O lipid quantification in NHEK after exposure to sterile conditioned 15% *C. acnes* supernatant or 8 mM PA after silencing *GPAT3*. Experiments conducted were performed at least in four replicates. **P* < 0.05, ***P* < 0.01, ****P* < 0.001, *****P* < 0.0001.

including lauric acid, palmitoleic acid isomer (C16:1Δ6), sphingosine, and dihydrosphingosine (*20*, *34*–*36*). Linoleic acid in NHEK lipid extract could partially explain the increased potency for *C. acnes* inhibition and has previously been shown to directly inhibit the growth of *C. acnes* (*37*). Furthermore, although not produced by the keratinocytes, *C. acnes* itself may also influence the overall composition of skin bacterial community as some SCFAs produced by *C. acnes* are antimicrobial and can inhibit biofilm formation by other organisms such as *S. epidermidis* (*17*, *34*). Furthermore, other commensal bacteria such as *Corynebacterium accolens*, a benign lipid-requiring species present in nostrils, can inhibit *pneumococcal* growth when supplemented with human skin surface TAGs thanks to a TAG lipase, LipS1, that hydrolyzes triolein into oleic acid (*38*). Thus, *C. acnes* is part of a complex and interconnected system on the skin that involves SCFA synthesis, induction of lipid synthesis, and cooperation with potential lipid metabolism by other microbes. More research is required to understand how the host and commensal microbes that regulate the final composition of health-associated skin microbiota.

C. acnes metabolizes TAGs into SCFAs under anaerobic conditions, and these molecules can act on mammalian cells by multiple mechanisms. *C. acnes* produces high amounts of propionic acid and other SCFAs, which creates a lipid-rich environment that is favorable for the growth and proliferation of the bacteria. One factor that can affect SCFA production by *C. acnes* is the availability of nutrients. In culture, the bacteria are grown under anaerobic conditions in nutrient-rich media that may optimize SCFA production while in vivo, sebum, which is a major nutrient source for *C. acnes* on the skin, is used by *C. acnes* for growth in the anaerobic environment of the hair follicle. The metabolic pathway by which *C. acnes* produces propionic acid appears to involve metabolism from pyruvate and methylmalonyl–coenzyme (CoA) by the methylmalonyl-CoA carboxyltransferase (*39*). However, the specific pathways involved in PA production in *C. acnes* are still being investigated, and available evidence suggests that *C. acnes* has a complex and multifaceted metabolism that contributes to its ability to colonize and persist in the skin microbiome (*39*, *40*). SCFA production is a key aspect of this metabolic activity.

Production of SCFA including propionic acid promotes an acidic environment that influences the survival of skin microbiota, formation of biofilms, as well as the function of pH-dependent enzymes required for lipid synthesis (*10*, *17*). A study of Shu *et al.* (*41*) have showed that the application of propionic acid on mice led to a significant decrease in the size of skin lesions infected with *S. aureus* USA300 and have direct antimicrobial activity against this pathogen. Another study showed the beneficial function of PA, they demonstrated that PA reduced UVB (Ultraviolet B)-induced functioning melanocyte levels by inhibiting tyrosinase activity in vitro and in vivo (*42*). Moreover, propionic acid has also anti-inflammatory effects in the gut and appears important toward

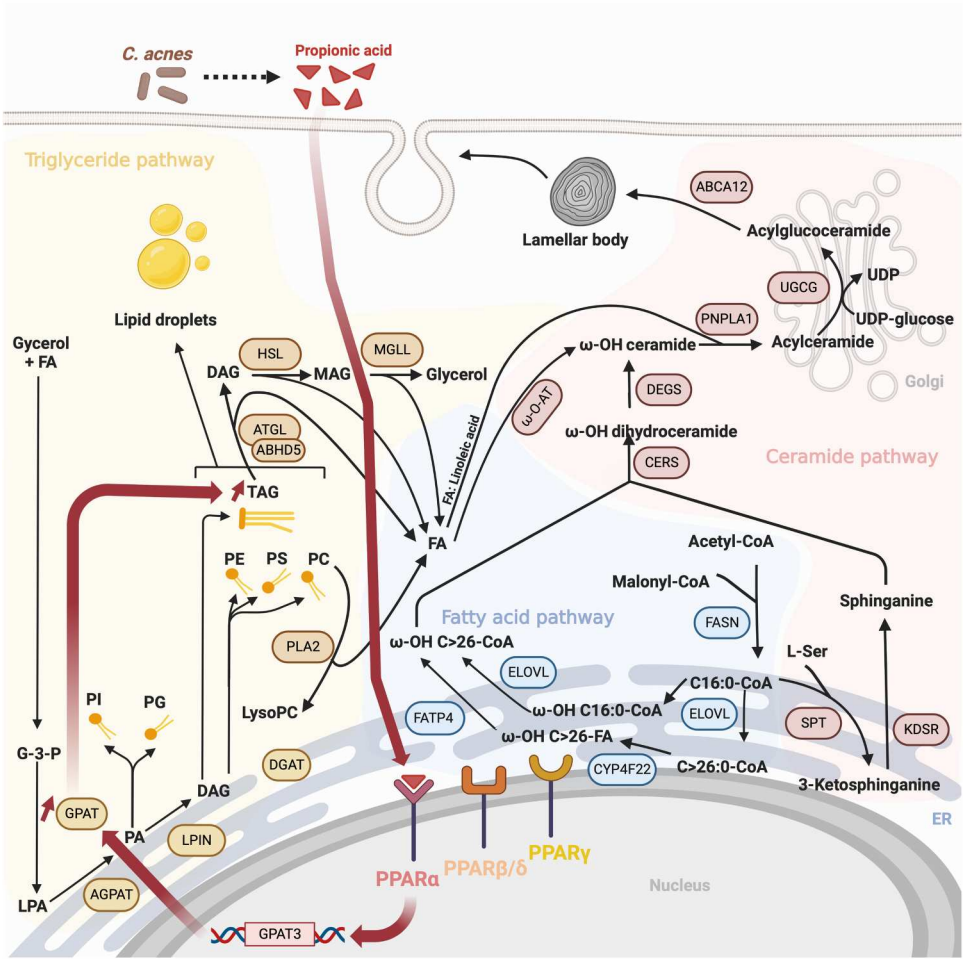

Fig. 6. Proposed model of the influence of *C. acnes* on triglyceride synthesis in NHEKs and relationship to other lipids that form the epidermal barrier. Illustration of lipid synthesis response to *C. acnes* SCFAs such as propionic acid. Dark red bold arrows show enzymatic steps and products induced by activation of PPARα. ER (Endoplasmic Reticulum), LPA (Lysophosphatidic acid), UDP (Uridine Diphosphate).

maintaining intestinal homeostasis (*43*). According to our results, propionic acid is a multifunctional molecule that can have numerous beneficial effects on skin barrier. However, while our studies on mice indicate a decrease in TEWL, acne patients demonstrated a significant increase in TEWL in comparison to healthy controls (*44*). Further research is needed to fully understand the switch that induces the development of acne by the bacteria. Previous studies have suggested a dose effect, as elevated concentrations of PA due to bacterial growth and metabolism may potentially lead to detrimental effects on the skin (*45*).

SCFA can also activate nuclear receptor PPARs (*23*), a function that has been extensively studied in relation to intestinal homeostasis. In the skin, PPARα is known to govern the expression of genes involved in lipid metabolism (*4*, *46*), and PPAR agonists have been shown to increase epidermal lipids and induce an improved permeability barrier in mouse skin (*24*, *46*, *47*). Our data provide physiological context to this observation by demonstrating how the most abundant bacterial skin commensal may contribute to skin barrier function by activating PPARs.

The association between improved epidermal barrier properties of cultured human keratinocytes or mouse skin in response to SCFAs produced by *C. acnes* is entirely consistent with the increased lipid production by keratinocytes we show here. However, other actions from these commensal bacteria may also contribute to improvement of the barrier. For example, two key barrier proteins, filaggrin and loricrin, were found to be increased in human reconstructed epidermis after treatment with *C. acnes* CM. Although these genes were not increased in NHEKs according the RNA-seq results, such findings support further investigation into the potential of *C. acnes* or other commensal skin bacteria to influence differentiation of keratinocytes.

The interactions between microbes and barrier tissues such as the skin are a complex network of many organisms, gene products, and functional responses. Here, we observed that *C. acnes* or its SCFA metabolites will induce a prominent increase in lipids in the epidermis, a response important for barrier formation and antimicrobial defense. These observations support the hypothesis that *C. acnes* co-evolved with humans as a mutualistic commensal that enhances the protective properties of the epidermis. Other commensal skin bacteria, such as *S. epidermidis*, have also been suggested to contribute to the preservation of the skin barrier by secreting a sphingomyelinase that is used by the host for ceramide synthesis

(*19*). It is conceivable that microbe-microbe and microbe-host interactions are both relevant to formation of the skin barrier. This information could be beneficial in treatment of patients with skin disorders and/or to restore a natural equilibrium of the skin microbiota. Further investigations are required to better understand the interactions between microbiota and the skin and the role of these responses in human health.

MATERIALS AND METHODS

Cell culture

Normal NHEKs (Thermo Fisher Scientific, Waltham, MA, C0015C) were cultured in EpiLife medium containing 60 μM $CaCl_2$ supplemented with 1× human keratinocyte growth supplement and 1× antibiotic antimycotic [PSA: Penicillin (100 U/ml), Streptomycin (100 U/ml), and Amphotericin B (250 ng/ml)] (Thermo Fisher Scientific, Waltham, MA). Cells were cultured in a 37°C, 5% CO_2 incubator. All experiments performed on NHEKs were between passages 3 and 5 and were grown to approximately 80% confluency followed by differentiation in high calcium (2 mM $CaCl_2$) EpiLife complete medium. For bacterial supernatant treatments, differentiated NHEKs were treated with the sterile-filtered bacterial supernatant at 10 or 15% by volume to EpiLife medium. Different concentrations of SCFAs butyric acid, acetic acid, isobutyric acid, and propionic acid (Sigma-Aldrich, St. Louis, MO); MALP-2 (100 ng/ml) (Enzo Life Sciences, Farmingdale, NY); HCl; and lyophilized *C. acnes* supernatant were applied to differentiated NHEK for 4 days.

Bacterial strains and culture

All *C. acnes* strains were grown on Brucella blood agar plates and grown for 3 days at 37°C under anaerobic conditions. Single-colony isolates were resuspended in 3 ml of reinforced clostridial medium (RCM) and grown for 3 days at 37°C under anaerobic conditions using BD GasPak EZ pouches (BD Biosciences). All the *Staphylococcus* strains were grown for 24 hours in tryptic soy broth at 300 rpm in an incubator at 37°C. The optical density at 600 nm was read to evaluate bacterial concentration. For in vitro experiments, bacteria were pelleted for 15 min, 4000 rpm at room temperature, and then all bacteria supernatants were filtered through a 0.22-μm filter. Sterile filtrate was then added to cultured cells. For in vivo experiments, *C. acnes* culture were pelleted, resuspended, and diluted in fresh RCM to approximately 1×10^7 colony-forming units (CFU). All bacteria strains used in this study are listed in Table 1.

Protein precipitation

Ammonium sulfate was added to 85% saturation, and the filtered supernatant was stirred gently at 4°C overnight before the precipitated protein was pelleted by centrifugation (5000*g* for 30 min at 4°C). The resulting protein pellet was dissolved in 2% ethanol in dH_2O. The proteins extracted were filtered by size 3 and 10 kDa by using centrifugal filter units (Sigma-Aldrich, St. Louis, MO; UFC500324 and UFC501024).

Oil Red O staining and quantification

An Oil Red O stock solution was prepared at 3 mg/ml in 100% isopropanol. Following stimulation, cells were washed three times with phosphate-buffered saline (PBS) and fixed in 10% formalin for 2 hours at room temperature. Cells were then rinsed with 60% isopropanol. Oil Red O working solution (60% diluted in dH_2O) was then applied to cells for 2 hours and 30 min. Then, cells were again rinsed three times with PBS. For Oil Red O quantification, 500 μl of 100% isopropanol per well of a 24-well plate was added for 5 min and then removed, and absorbance at 510 nm was measured. Absorbance values were normalized to the number of cells counted by trypan blue after trypsinization, and fold change was determined after treatment.

RNA isolation and qPCR

RNA was extracted from cultured cells after 4 days using the PureLink Isolation kit (Thermo Fisher Scientific, Waltham, MA; 12183025). Purified RNA (up to 1 μg) was used to synthesize cDNA using the iScript cDNA Synthesis Kit (Bio-Rad, USA). Quantitative real-time PCR was performed with the CFX96 Real-Time System (Bio-Rad) using SYBR Green Mix (Bimake, Houston, TX). The housekeeping gene *Gapdh* was used to normalize gene expression in samples. The sequences of the primers are shown in Table 2. All primers including the primers "Hs.PT.58" were provided by Integrated DNA Technologies.

RNA sequencing

NHEK cells were treated with 8 mM propionic acid or with 15% of *C. acnes* supernatant or RCM (control) for 4 days in triplicate. Then, RNA was extracted using the PureLink RNA mini kit. Isolated RNA was submitted to the University of California, San Diego (UCSD) Institute for Genomic Medicine (IGM) Center for RNA-seq performed on a high-output run V4 platform (Illumina, USA) with a single read 100 cycle runs. Reads were aligned to a human reference genome (hg38) using STAR, and a counts table was generated using featureCounts. Normalization and differential expression analysis was performed using DESeq2. Heatmaps and PCA plots were generated using Variance Stabilizing Transformation (VST)–normalized data and pheatmap and plotPCA packages, respectively.

PPARs inhibitors and gene silencing by siRNA

Inhibitors of PPARs PPARα (GW6471), PPARβ/δ (GSK3787), and PPARγ (T0070907) were used at different concentrations and were added in NHEKs 1 hour before adding RCM (control), 15% of *C. acnes* supernatant, or 8 mM propionic acid for 4 days. Silencer select siRNA PPARα (s10880), siRNA PPARβ/δ (s10884), siRNA PPARγ (s10887), siRNA GPAT3 (s39444), siRNA FFAR2 (s6082), and siRNA FFAR3 (s6078) were used in keratinocytes according to the manufacturer's instructions (Thermo Fisher Scientific, Waltham, MA). Briefly, NHEKs were transfected by addition of transfection mixture with a final siRNA concentration of 10 nM and a final Lipofectamine concentration of 2.5 μl/ml. siRNA was applied to keratinocyte cultures for 18 hours, after which fresh medium was added to cells for 24 hours before further stimulation. As a control, nontargeting control siRNA (Thermo Fisher Scientific, Waltham, MA; AM4611) was transfected in the same procedure. Cells were incubated for 4 days at 37°C, and the efficiency of knockdown was evaluated by reverse transcription PCR.

Lipid extraction and antimicrobial assays

After exposure to 8 mM propionic acid or 15% of *C. acnes* supernatant or RCM (control) for 4 days, lipids from 4 million NHEKs were

Table 1. Bacterial strains used in this study.

Name
Cutibacterrium acnes ATCC6919 - phylotype IA1
Cutibacterrium acnes 17 - phylotype IB
Cutibacterrium acnes 21 - phylotype II
Cutibacterrium acnes 35 - phylotype II
Cutibacterrium acnes 42 - phylotype IA1
Cutibacterrium acnes 46 - phylotype IA1
Cutibacterrium acnes 61 - phylotype IA1
Staphylococcus epidermidis 14990
Staphylococcus aureus 113
Staphylococcus warneri ATCC 49454
Staphylococcus hominis C2
Staphylococcus hominis A9

extracted using chloroform:methanol:water at the ratio 2:1:1. Then, the samples were centrifuged at 700 rcf (relative centrifugal force) for 1 min, and the lower phase was collected and blew off with nitrogen gaz. Then, the dried extracts were resuspended in 5% chloroform diluted in PBS. *C. acnes* was cultured in RCM at 37°C during 3 days in an anaerobic condition. For antimicrobial assays, the bacteria were inoculated at a concentration of 1×10^4 CFU/ml into a 96-well round-bottom plate containing a serial dilution of extracted lipid from NHEKs in RCM or with difference concentration of PA. The arbitrary units of 1 correspond to the lipid extract from 4 million NHEKs. Then, the number of CFU was enumerated into agar plate at dedicated days.

Keratinocyte paracellular permeability

NHEKs were plated into Transwell inserts (Costar, 3470) at 3×10^5 cells/ml and were grown to approximately 80% confluency followed by differentiation in high calcium (2 mM $CaCl_2$) EpiLife complete medium. After exposure to RCM (control), 15% of *C. acnes* supernatant, or 8 mM propionic acid for 1 day, an FD-4 solution (1.25 mg/ml) was added to the upper chamber.

Then, samples were collected from the lower chamber after 1 hour and 30 min. The amount of FD-4 that had diffused from the apical to the basal side of the filter was measured at the excitation/emission wavelengths of 490/510 nm. Relative fluorescence flux = experimental condition/media alone × 100.

Reconstructed human epidermis

Reconstructed human epidermis was obtained by seeding 3×10^5 NHEKs into culture inserts (Sigma-Aldrich, St. Louis, MO; PIHP01250). Cells were cultured submerged in complete EpiLife medium with 2 mM Ca^{2+} (Thermo Fisher Scientific, Waltham, MA). After 1 day, the cultures were then raised to the air-liquid interface, and the lower chamber was replaced by complete EpiLife medium with 2 mM Ca^{2+} + vitamin C (75 µg/ml; A8960) + KGF (Keratinocyte Growth Factor) (10 ng/ml; K1757) (Sigma-Aldrich, St. Louis, MO). The cultures were grown for an additional 12 days, and the medium of the lower chamber was replaced every 2 days. Then, 40 µl of 15% *C. acnes* supernatant or RCM in PBS

Table 2. Primers used for qPCR.

Gene name	Sequences
ABCA12	F-TCTTTTCTTCGCAATGGTTCCT R-GCTGGCATGACTTCTCTATCAAA
ABHD5	Hs.PT.58.27919187
AGPAT1	Hs.PT.58.24287326
AGPAT2	Hs.PT.58.38804900
AGPAT3	Hs.PT.58.208776
AGPAT4	Hs.PT.58.194257
AGPAT6	Hs.PT.58.14663523
PNPLA2/ ATGL	Hs.PT.58.45404013
CERS3	F-TGGACGCAGACCTGTAACACCC R-AGGCTCGAGGTGATACATAGGCA
CERS4	Hs.PT.58.24838321
DEGS1	Hs.PT.58.27518549
DEGS2	F-CGGCGCAAGGAGATACTGG R-GTTGTGCGAGATGTCGTGGA
DGAT1	Hs.PT.58.39709623
DGAT2	Hs.PT.58.39763042
ELOVL1	Hs.PT.58.40582025.g
ELOVL3	Hs.PT.58.39205875
ELOVL4	F-ATGTGACCATTGGGCACACG R-GGCAATTAGAGCCCAGTGCAT
ELOVL6	Hs.PT.58.1453354
FADS1	Hs.PT.58.14503404
FADS2	Hs.PT.58.14822907
FASN	F-CCCCTGATGAAGAAGGATCA R-ACTCCACAGGTGGGAACAAG
SLC27A4/ FATP4	Hs.PT.58.23105929
FFAR2	F - TGCTACGAGAACTTCACCGAT R-GGAGAGCATGATCCACACAAAAC
FFAR3	F - TTCACCACCATCTATCTCACCG R-GGAACTCCAGGTAGCAGGTC
FLG	F-GGATCCTCTCACCGCGATAC R-GCCTTTCAGTGCCCTCAGAT
GPAM	Hs.PT.58.20958744
GPAT3	Hs.PT.58.1668782
LIPE/HSL	Hs.PT.58.39451694
IFNB1	F-ATGACCAACAAGTGTCTCCTCC R-GGAATCCAAGCAAGTTGTAGCTC
IVL	F-GATGTCCCAGCAACACACAC R-TGCTCACATTCTTGCTCAGG
KDSR	Hs.PT.58.40263528
KLK5	F-AGAGCATGTTCTCGCCAACAA R-TGGGTGTGCATATCGCAGTC
LOR	F-GGAGTTGGAGGTGTTTTCCA R-ACTGGGGTTGGGAGGTAGTT
LPIN1	Hs.PT.58.39304832
LPIN2	Hs.PT.58.28172771

continued on next page

Gene name	Sequences
LPIN3	Hs.PT.58.3370125
MGLL	Hs.PT.58.40304258
NR1H2	Hs.PT.58.22966325
NR1H3	Hs.PT.58.39933583
PNPLA1	Hs.PT.58.40111376
PPARα	F-GCAGAAACCCAGAACTCAGC R-ATGGCCCAGTGTAAGAAACG
PPARβ/δ	F-AGGAGCCATTCTGTGTGTGA R-TCCTGCCAGCAGAGAGTGAT
PPARγ	F-GCTGTGCAGGAGATCACAGA R-GGGCTCCATAAAGTCACCAA
RXRA	Hs.PT.58.39268112
SCD	Hs.PT.58.45714389
SPTLC2	F-AACGGGGAAGTACGGAACG R-CCCCACATACGTGAGCACAG
UGCG	F-GTGTTGGATCAAGCAGGAGGACT R-TGCAAACCTCCAACCTCGGTCA

was added at the surface of the reconstructed epidermis and left for 2 hours once a day for 4 days.

Mouse experiments

All animal experiments were approved by the UCSD Institutional Animal Care and Use Committee. SKH-1 hairless mice were purchased from The Jackson Laboratory, bred, and maintained in animal facility of UCSD. One hundred microliters of squalene (Sigma-Aldrich, St. Louis, MO) was topically applied to the backs of age-matched (8 to 10 weeks) SKH-1 mice 24 hours before contact to *C. acnes* and every 24 hours thereafter throughout the duration of the experiment. Mice were intradermally injected with approximately 1×10^7 CFU of *C. acnes* or control (PBS) or applied topically at 1×10^7 CFU/cm^2 on a piece of sterile gauze. A bio-occlusive dressing (Tegaderm; 3M) along with a flexible fabric Band-Aid was applied on top of gauze to hold in place for 24 hours. On day 4, mice were euthanized, and a skin biopsy was performed. For the TEWL measurement, a TEWL measuring device was placed on the back skin of tape-stripped mice after applying 100 μl of *C. acnes* supernatant or 8 mM propionic acid topically. TEWL measurements were then taken at regular intervals over a specific duration. The TEWL in g/m^2/hour was normalized to the TEWL measurement corresponding to the tape-stripped mice before topical application and is expressed in percentage (%).

Histology and immunofluorescence

Skin samples were then embedded in Tissue-Tek optimal cutting temperature (OCT) for tissue sectioning (8-μm thick at 20°C using a Leica CM1860 cryostat) for histological or immunofluorescent analyses. Frozen tissue sections were stained with primary antibodies overnight at 4°C, secondary antibodies for 1 hour at room temperature, and nuclei were counterstained with 4′,6-diamidino-2-phenylindole. Bodipy solution (Thermo Fisher Scientific, Waltham, MA) was used to visualize lipid droplets. All images were taken with an Olympus BX41 microscope. Fluorescence quantification of loricrin and filaggrin was accomplished by using ImageJ software, which involved measuring the fluorescence within a defined surface area specific to the localization of each protein on multiple images.

DMS-based shotgun lipidomics

Mouse skin samples were treated with dispase (5 U/ml) (Sigma-Aldrich, St. Louis, MO, D4693) overnight to separate the epidermis to the dermis, and the epidermis was weighted (50 to 100 mg). Then, the epidermis was collected in a 2-ml homogenizer tube preloaded with 2.8-mm ceramic beads (Omni, 19-628). Then, 0.75 ml of PBS was added to the tube and homogenized in the Omni Bead Ruptor Elite (3 cycles of 10 s at 5m/s with a 10-s dwell time). Homogenate containing 2 to 6 mg of original tissue was transferred to a glass tube for extraction. One to 2 million of NHEKs were collected in a glass tube after trypsinization and enumerated. Then, a modified Bligh and Dyer extraction (*48*) was carried out on all samples. Before biphasic extraction, an internal standard mixture consisting of 70 lipid standards across 17 subclasses was added to each sample (AB Sciex 5040156, Avanti 330827, Avanti 330830, Avanti 330828, and Avanti 791642). Following two successive extractions, pooled organic layers were dried down in a Thermo SpeedVac SPD300DDA using ramp setting 4 at 35°C for 45 min with a total run time of 90 min. Lipid samples were resuspended in 1:1 methanol/dichloromethane with 10 mM ammonium acetate and transferred to robovials (Thermo Fisher Scientific, 10800107) for analysis. Samples were analyzed on the Sciex 5500 with DMS device (Lipidyzer platform) with an expanded targeted acquisition list consisting of 1450 lipid species across 17 subclasses. Differential mobility device on Lipidyzer was tuned with EquiSPLASH LIPIDOMIX (Avanti 330731). Data analysis was performed on an in-house data analysis platform comparable to the Lipidyzer Workflow Manager (*49*). The instrument method including settings, tuning protocol, and multiple reaction monitoring (MRM) list is available in (*49*). Quantitative values were normalized to milligrams of tissue and to numbers of cells.

Determination of SCFA concentrations by LC-MS

SCFAs (acetic acid, propionic acid, butyric acid, ^{13}C4-butyric acid, isobutyric acid, 2-methylbutanoic acid, valeric acid, isovaleric acid, 3-methylvaleric acid, 4-metylvaleric acid, and hexanoic acid) were purchased from Sigma-Aldrich. Analytical reagent-grade 3-nitrophenylhydrazine hydrochloride (3NPH, 98%), *N*-(3-dimethylaminopropyl)-*N*′-ethylcarbodiimide (EDC, 97%), and high-performance liquid chromatography–grade pyridine were also purchased from Sigma-Aldrich. Deuterated (d7) butyric acid and heavy carbon 3-nitrophenylhydrazine hydrochloride ($^{13}C_6$-3NPH, 98%) were purchased from Cayman Chemical.

SCFAs were derivatized according to Han *et al.* (*50*). An isotope-labeled internal standard mix was prepared by adding 50 μl of standard mix (4 mM acetic acid, 2 mM propionic acid, 2 mM d7-butyric acid, and 1 mM of the other 8 SCFAs), 25 μl of 120 mM EDC in 50% acetonitrile (ACN), and 25 μl of 6% pyridine in 50% ACN to 1 mg of $^{13}C_6$-3NPH. The mixture was reached at 40°C for 30 min and diluted 200-fold in 10% ACN for use. Media samples were diluted 1:1 in ACN, vortexed, and centrifuged. Samples (40 μl) were mixed with 5 μl of 250 μM ^{13}C4-butyric acid and sequentially mixed with 20 μl of 200 mM 3NPH in 50% ACN and 20 μl of 120 mM EDC in 50% ACN containing 6% pyridine. Mixtures were incubated at 40°C

Table 3. MRM transitions in negative mode for derivatized SCFAs. *m/z*, mass/charge ratio.

Analyte	Retention time (min)	Ionization mode	MRM transition (*m/z*)
Acetate	2.9	Negative	194.2 → 137.1
			194.2 → 152.1
Propionate	4.5	Negative	208.1 → 137.1
			208.1 → 165.1
Isobutyrate	6.5	Negative	222.1 → 137.1
			222.1 → 152.1
Butyrate	6.8	Negative	222.1 → 137.1
			222.1 → 152.1
Isovalerate	9.0	Negative	236.2 → 137.1
			236.2 → 152.1
Valerate	9.5	Negative	236.2 → 137.1
			236.2 → 152.1

for 30 min. After reaction, samples were cooled on ice for 1 min and diluted with 915 μl of 10% ACN. An SCFA standard curve mix containing 50 μM of each standard (40 μl) was mixed with 5 μl of 250 μM ^{13}C4-butyric acid (internal standard) and derivatized as described above. Media samples and standard curve were mixed 1:1 with isotope-labeled internal standard mix before LC-MS analysis.

Derivatized SCFAs were analyzed on a Dionex Ultimate 3000 LC system (Thermo Fisher Scientific) coupled to a TSQ Quantiva mass spectrometer (Thermo Fisher Scientific) fitted with a Kinetex C18 reversed phase column (1.7 μm, 150 mm × 2.1 mm, Phenomenex). The following LC solvents were used: solution A, 0.1% formic acid in water, solution B, 0.1% formic acid in ACN. At the flow rate of 0.25 ml/min, the following reversed phase gradient was used: 20% B for 2 min, 20 to 50% B in 12 min, up to 100% B in 0.1 min, 100% B for 4 min, and re-equilibrated to 20% B for 4 min, for a total run time of 22 min. The column oven temperature was set to 35°C, the autosampler was kept at 4°C, and injection volume was 10 μl. MS analysis was performed using electrospray ionization in negative ion mode, with spray voltage of −3 kV, ion transfer tube temperature of 325°C, and vaporizer temperature of 275°C. MRM was performed by using mass transitions of parent ions into corresponding fragment ions for each analyte (Table 3). Peak areas for each derivatized SCFA were extracted using Skyline (5) and normalized by each specific internal standard. SCFA concentrations were calculated using normalized standard curves.

Human skin sample collection

Adult human skin biopsies, from the back of healthy donors (age 18 to 50), were collected from the Dermatology Clinic, UCSD. Sample acquisitions were approved and regulated by the UCSD Institutional Review Board (reference number 140144). Written informed consent was obtained from all subjects. Biopsies were immediately embedded in OCT compound for sectioning and staining.

Statistical analysis

Experiments conducted were performed at least in triplicate. Significant differences between the means of the different treatments were evaluated using GraphPad Prism version 9.4.1 (GraphPad Software Inc., La Jolla, CA). Statistical significance was calculated using a one-way analysis of variance (ANOVA) with Tukey's multiple comparisons test and Student's two-tailed *t* test, where $^{*}P < 0.05$, $^{**}P < 0.01$, $^{***}P < 0.001$, and $^{****}P < 0.0001$.

Supplementary Materials

This PDF file includes:
Figs. S1 to S7
Legend for table S1

Other Supplementary Material for this manuscript includes the following:
Table S1

REFERENCES AND NOTES

1. P. M. Elias, Structure and function of the stratum corneum permeability barrier. *Drug Dev. Res.* **13**, 97–105 (1988).
2. G. K. Menon, G. W. Cleary, M. E. Lane, The structure and function of the stratum corneum. *Int. J. Pharm.* **435**, 3–9 (2012).
3. T. A. Harris-Tryon, E. A. Grice, Microbiota and maintenance of skin barrier function. *Science* **376**, 940–945 (2022).
4. K. R. Feingold, Y. J. Jiang, The mechanisms by which lipids coordinately regulate the formation of the protein and lipid domains of the stratum corneum. *Dermatoendocrinol.* **3**, 113–118 (2011).
5. B. MacLean, D. M. Tomazela, N. Shulman, M. Chambers, G. L. Finney, B. Frewen, R. Kern, D. L. Tabb, D. C. Liebler, M. J. MacCoss, Skyline: An open source document editor for creating and analyzing targeted proteomics experiments. *Bioinformatics* **26**, 966–968 (2010).
6. F. F. Sahle, T. Gebre-Mariam, B. Dobner, J. Wohlrab, R. H. H. Neubert, Skin diseases associated with the depletion of stratum corneum lipids and stratum corneum lipid substitution therapy. *Skin Pharmacol. Physiol.* **28**, 42–55 (2015).
7. B. L. Lew, Y. Cho, J. Kim, W. Y. Sim, N. I. Kim, Ceramides and cell signaling molecules in psoriatic epidermis: Reduced levels of ceramides, PKC-alpha, and JNK. *J. Korean Med. Sci.* **21**, 95–99 (2006).
8. J. Ishikawa, H. Narita, N. Kondo, M. Hotta, Y. Takagi, Y. Masukawa, T. Kitahara, Y. Takema, S. Koyano, S. Yamazaki, A. Hatamochi, Changes in the ceramide profile of atopic dermatitis patients. *J. Invest. Dermatol.* **130**, 2511–2514 (2010).
9. T. Yoshida, L. A. Beck, A. De Benedetto, Skin barrier defects in atopic dermatitis: From old idea to new opportunity. *Allergol. Int.* **71**, 3–13 (2022).
10. G. J. M. Christensen, H. Brüggemann, Bacterial skin commensals and their role as host guardians. *Benef. Microbes* **5**, 201–215 (2014).
11. M. Allhorn, S. Arve, H. Brüggemann, R. Lood, A novel enzyme with antioxidant capacity produced by the ubiquitous skin colonizer propionibacterium acnes. *Sci. Rep.* **6**, 36412 (2016).
12. S. M. Tuchayi, E. Makrantonaki, R. Ganceviciene, C. Dessinioti, S. R. Feldman, C. C. Zouboulis, Acne vulgaris. *Nat. Rev. Dis. Primers* **1**, 15029 (2015).
13. J. A. Sanford, A. M. O'Neill, C. C. Zouboulis, R. L. Gallo, Short-chain fatty acids from *Cutibacterium acnes* activate both a canonical and epigenetic inflammatory response in human sebocytes. *J. Immunol.* **202**, 1767–1776 (2019).
14. Y.-C. Huang, C.-H. Yang, T.-T. Li, C. C. Zouboulis, H.-C. Hsu, Cell-free extracts of propionibacterium acnes stimulate cytokine production through activation of p38 MAPK and Toll-like receptor in SZ95 sebocytes. *Life Sci.* **139**, 123–131 (2015).
15. I. Nagy, A. Pivarcsi, K. Kis, A. Koreck, L. Bodai, A. McDowell, H. Seltmann, S. Patrick, C. C. Zouboulis, L. Kemény, Propionibacterium acnes and lipopolysaccharide induce the expression of antimicrobial peptides and proinflammatory cytokines/chemokines in human sebocytes. *Microbes Infect.* **8**, 2195–2205 (2006).
16. M. Yang, M. Zhou, L. Song, A review of fatty acids influencing skin condition. *J. Cosmet. Dermatol.* **19**, 3199–3204 (2020).
17. K. Nakamura, A. M. O'Neill, M. R. Williams, L. Cau, T. Nakatsuji, A. R. Horswill, R. L. Gallo, Short chain fatty acids produced by Cutibacterium acnes inhibit biofilm formation by Staphylococcus epidermidis. *Sci. Rep.* **10**, 21237 (2020).
18. F. P. W. Radner, J. Fischer, The important role of epidermal triacylglycerol metabolism for maintenance of the skin permeability barrier function. *Biochim. Biophys. Acta* **1841**, 409–415 (2014).

19. Y. Zheng, R. L. Hunt, A. E. Villaruz, E. L. Fisher, R. Liu, Q. Liu, G. Y. C. Cheung, M. Li, M. Otto, Commensal Staphylococcus epidermidis contributes to skin barrier homeostasis by generating protective ceramides. *Cell Host Microbe* **30**, 301–313 (2022).
20. D. R. Drake, K. A. Brogden, D. V. Dawson, P. W. Wertz, Thematic Review Series: Skin Lipids. Antimicrobial lipids at the skin surface. *J. Lipid Res.* **49**, 4–11 (2008).
21. M. Akiyama, Acylceramide is a key player in skin barrier function: Insight into the molecular mechanisms of skin barrier formation and ichthyosis pathogenesis. *FEBS. J.* **288**, 2119–2130 (2021).
22. A. De Benedetto, N. M. Rafaels, L. Y. McGirt, A. I. Ivanov, S. N. Georas, C. Cheadle, A. E. Berger, K. Zhang, S. Vidyasagar, T. Yoshida, M. Boguniewicz, T. Hata, L. C. Schneider, J. M. Hanifin, R. L. Gallo, N. Novak, S. Weidinger, T. H. Beaty, D. Y. Leung, K. C. Barnes, L. A. Beck, Tight junction defects in patients with atopic dermatitis. *J. Allergy Clin. Immunol.* **127**, 773–786.e7 (2011).
23. S. Alex, K. Lange, T. Amolo, J. S. Grinstead, A. K. Haakonsson, E. Szalowska, A. Koppen, K. Mudde, D. Haenen, S. Al-Lahham, H. Roelofsen, R. Houtman, B. van der Burg, S. Mandrup, A. M. Bonvin, E. Kalkhoven, M. Müller, G. J. Hooiveld, S. Kersten, Short-chain fatty acids stimulate angiopoietin-like 4 synthesis in human colon adenocarcinoma cells by activating peroxisome proliferator-activated receptor γ. *Mol. Cell. Biol.* **33**, 1303–1316 (2013).
24. B. Lu, Y. J. Jiang, P. Kim, A. Moser, P. M. Elias, C. Grunfeld, K. R. Feingold, Expression and regulation of GPAT isoforms in cultured human keratinocytes and rodent epidermis. *J. Lipid Res.* **51**, 3207–3216 (2010).
25. J. A. Sanford, L.-J. Zhang, M. R. Williams, J. A. Gangoiti, C.-M. Huang, R. L. Gallo, Inhibition of HDAC8 and HDAC9 by microbial short-chain fatty acids breaks immune tolerance of the epidermis to TLR ligands. *Sci. Immunol.* **1**, eaah4609 (2016).
26. C. Lefèvre, F. Jobard, F. Caux, B. Bouadjar, A. Karaduman, R. Heilig, H. Lakhdar, A. Wollenberg, J.-L. Verret, J. Weissenbach, M. Özgüc, M. Lathrop, J.-F. Prud'homme, J. Fischer, Mutations in CGI-58, the gene encoding a new protein of the esterase/lipase/thioesterase subfamily, in chanarin-dorfman Syndrome. *Am. J. Hum. Genet.* **69**, 1002–1012 (2001).
27. J. Fischer, C. Lefèvre, E. Morava, J.-M. Mussini, P. Laforêt, A. Negre-Salvayre, M. Lathrop, R. Salvayre, The gene encoding adipose triglyceride lipase (PNPLA2) is mutated in neutral lipid storage disease with myopathy. *Nat. Genet.* **39**, 28–30 (2007).
28. S. J. Stone, H. M. Myers, S. M. Watkins, B. E. Brown, K. R. Feingold, P. M. Elias, R. V. Farese Jr., Lipopenia and skin barrier abnormalities in DGAT2-deficient mice. *J. Biol. Chem.* **279**, 11767–11776 (2004).
29. Y. Uchida, Y. Cho, S. Moradian, J. Kim, K. Nakajima, D. Crumrine, K. Park, M. Ujihara, M. Akiyama, H. Shimizu, W. M. Holleran, S. Sano, P. M. Elias, Neutral lipid storage leads to acylceramide deficiency, likely contributing to the pathogenesis of Dorfman–Chanarin syndrome. *J. Invest. Dermatol.* **130**, 2497–2499 (2010).
30. S. Li, M. Villarreal, S. Stewart, J. Choi, G. Ganguli-Indra, D. C. Babineau, C. Philpot, G. David, T. Yoshida, M. Boguniewicz, J. M. Hanifin, L. A. Beck, D. Y. Leung, E. L. Simpson, A. K. Indra, Altered composition of epidermal lipids correlates with Staphylococcus aureus colonization status in atopic dermatitis. *Br. J. Dermatol.* **177**, e125–e127 (2017).
31. M. Ujihara, K. Nakajima, M. Yamamoto, M. Teraishi, Y. Uchida, M. Akiyama, H. Shimizu, S. Sano, Epidermal triglyceride levels are correlated with severity of ichthyosis in dorfman-chanarin syndrome. *J. Dermatol. Sci.* **57**, 102–107 (2010).
32. M. Ottaviani, E. Camera, M. Picardo, Lipid mediators in acne. *Mediators Inflamm.* **2010**, 858176 (2010).
33. X. Li, C. He, Z. Chen, C. Zhou, Y. Gan, Y. Jia, A review of the role of sebum in the mechanism of acne pathogenesis. *J. Cosmet. Dermatol.* **16**, 168–173 (2017).
34. T. Nakatsuji, M. C. Kao, L. Zhang, C. C. Zouboulis, R. L. Gallo, C. M. Huang, Sebum free fatty acids enhance the innate immune defense of human sebocytes by upregulating beta-defensin-2 expression. *J. Invest. Dermatol.* **130**, 985–994 (2010).
35. J. J. Wille, A. Kydonieus, Palmitoleic acid isomer (C16:1delta6) in human skin sebum is effective against gram-positive bacteria. *Skin Pharmacol. Appl. Skin Physiol.* **16**, 176–187 (2003).
36. B. K. Yoon, J. A. Jackman, E. R. Valle-González, N.-J. Cho, Antibacterial free fatty acids and monoglycerides: Biological activities, experimental testing, and therapeutic applications. *Int. J. Mol. Sci.* **19**, 1114 (2018).
37. M. Z. Sultan, K.-M. Lee, S. S. Moon, Antibacterial effect of naturally occurring unsaturated fatty acids from Prunus Japonica against Propionibacterium acnes. *Orient. Pharm. Exp. Med.* **9**, 90–96 (2009).
38. L. Bomar, S. D. Brugger, B. H. Yost, S. S. Davies, K. P. Lemon, Corynebacterium accolens releases antipneumococcal free fatty acids from human nostril and skin surface triacylglycerols. *MBio* **7**, e01725–e01715 (2016).
39. H. Brüggemann, Insights in the pathogenic potential of Propionibacterium acnes from its complete genome. *Semin. Cutan. Med. Surg.* **24**, 67–72 (2005).
40. S. Fitz-Gibbon, S. Tomida, B. H. Chiu, L. Nguyen, C. Du, M. Liu, D. Elashoff, M. C. Erfe, A. Loncaric, J. Kim, R. L. Modlin, J. F. Miller, E. Sodergren, N. Craft, G. M. Weinstock, H. Li, Propionibacterium acnes strain populations in the human skin microbiome associated with acne. *J. Invest. Dermatol.* **133**, 2152–2160 (2013).
41. M. Shu, Y. Wang, J. Yu, S. Kuo, A. Coda, Y. Jiang, R. L. Gallo, C.-M. Huang, Fermentation of Propionibacterium acnes, a commensal bacterium in the human skin microbiome, as skin probiotics against methicillin-resistant Staphylococcus aureus. *PLOS ONE* **8**, e55380 (2013).
42. H.-J. Kao, Y.-H. Wang, S. Keshari, J. J. Yang, S. Simbolon, C.-C. Chen, C.-M. Huang, Propionic acid produced by Cutibacterium acnes fermentation ameliorates ultraviolet B-induced melanin synthesis. *Sci. Rep.* **11**, 11980 (2021).
43. C. Martin-Gallausiaux, L. Marinelli, H. M. Blottière, P. Larraufie, N. Lapaque, SCFA: Mechanisms and functional importance in the gut. *Proc. Nutr. Soc.* **80**, 37–49 (2021).
44. L. Zhou, X. Liu, X. Li, X. He, X. Xiong, J. Lai, Epidermal barrier integrity is associated with both skin microbiome diversity and composition in patients with acne vulgaris. *Clin. Cosmet. Investig. Dermatol.* **15**, 2065–2075 (2022).
45. G. Tax, E. Urbán, Z. Palotás, R. Puskás, Z. Kónya, T. Bíró, L. Kemény, K. Szabó, Propionic acid produced by propionibacterium acnes strains contri-butes to their pathogenicity. *Acta Derm. Venereol.* **96**, 43–49 (2016).
46. M. Rivier, I. Castiel, I. Safonova, G. Ailhaud, S. Michel, Peroxisome proliferator-activated receptor-α enhances lipid metabolism in a skin equivalent model. *J. Invest. Dermatol.* **114**, 681–687 (2000).
47. M.-Q. Man, E.-H. Choi, M. Schmuth, D. Crumrine, Y. Uchida, P. M. Elias, W. M. Holleran, K. R. Feingold, Basis for improved permeability barrier homeostasis induced by PPAR and LXR activators: Liposensors stimulate lipid synthesis, lamellar body secretion, and post-secretory lipid processing. *J. Invest. Dermatol.* **126**, 386–392 (2006).
48. W.-Y. Hsieh, K. J. Williams, B. Su, S. J. Bensinger, Profiling of mouse macrophage lipidome using direct infusion shotgun mass spectrometry. *STAR Protoc.* **2**, 100235 (2020).
49. B. Su, L. F. Bettcher, W. Y. Hsieh, D. Hornburg, M. J. Pearson, N. Blomberg, M. Giera, M. P. Snyder, D. Raftery, S. J. Bensinger, K. J. Williams, A DMS shotgun lipidomics workflow application to facilitate high-throughput, comprehensive lipidomics. *J. Am. Soc. Mass Spectrom.* **32**, 2655–2663 (2021).
50. J. Han, K. Lin, C. Sequeira, C. H. Borchers, An isotope-labeled chemical derivatization method for the quantitation of short-chain fatty acids in human feces by liquid chromatography-tandem mass spectrometry. *Anal. Chim. Acta* **854**, 86–94 (2015).

Acknowledgments: We thank A. Pinto and C. Aguilera for technical support. **Funding:** This work was supported by National Institutes of Health P50AR080594, R01AR074302, R37AI052453, U01AI152038, and R01AR076082 (to R.L.G) and P50AR080594 and P01 HL146358 (to S.J.B). SCFA composition analysis was supported by the Mass Spectrometry Core of the Salk Institute with funding from NIH-NCI CCSG: P30 014195 and the Helmsley Center for Genomic Medicine. **Author contributions:** R.L.G. and S.A. conceived the experiments. S.A. carried out the experiments. R.L.G. and S.A. wrote the manuscript with input from all authors. L.C. and A.M.O. helped to conceive experiments. K.C. helped for RNA-seq analysis. F.L. and A.R.-M. assisted in staining and assays for antimicrobial activity. K.J.W. and S.J.B. performed the lipidomic analysis. L.C., B.C., and C.M. provided protocols and advice for the project. R.L.G. conceived the original idea and supervised the project. **Competing interests:** R.L.G. is a co-founder, scientific advisor, consultant, and has equity in MatriSys Biosciences. All other authors declare that they have no competing interests. **Data and materials availability:** All data needed to evaluate the conclusions in the paper are present in the paper and/or the Supplementary Materials. Sequencing data from normal human epidermal keratinocytes treated with *C. acnes* 6919 CM, and propionic acid has been deposited to Dryad (doi: 10.5061/dryad.8cz8w9gvq).

Submitted 11 January 2023
Accepted 20 July 2023
Published 18 August 2023
10.1126/sciadv.adg6262